EXPERIMENTAL INVESTIGATION OF TEXTILE PERMEABILITY IN THE PRESENCE OF SPHERICAL INCLUSIONS

B. Caglar[1,2], V. Michaud[2] and E. M. Sozer[1]

[1]*Mechanical Engineering Department, Koc University, Rumelifeneri Yolu, Sariyer 34450, Istanbul, Turkey*
[2]*Laboratoire de Technologie des Composites et Polymères (LTC), Ecole Polytechnique Fédérale de Lausanne (EPFL), Station 12, Lausanne CH-1015, Switzerland*
bacaglar@ku.edu.tr, veronique.michaud@epfl.ch, msozer@ku.edu.tr

Keywords: Permeability, textile, effects of inclusions, capillary effects

Abstract

Addition of a third material phase to a resin and reinforcement system is a favored approach to tailor properties and features of composite materials, including but not limited to the ease of stacking and preforming, or healing ability. This addition changes the structure of the empty spaces between the reinforcing fibers and thus the overall permeability is affected. In this study, the effect of model rigid spherical inclusions on the permeability of woven textiles is investigated. Several diameter ranges of glass beads (40.0-70.0, 70.0-100, 100-200, 200-300, 300-400, and 400-800 μm) with a volume fraction of 5.0% are manually sieved between the layers of a plain weave glass textile, which has a bundle-interstice gap in 150-200 μm range. Experiments are repeated for 2.5 and 10% volume fractions for three diameter ranges (40.0-70.0, 100-200, and 400-800 μm) to investigate the influence of the concentration of inclusions on permeability. Experimental results show that an increase in the diameter or an increase in the volume fraction of the rigid inclusions causes a non-monotonic change in permeability. For all diameter ranges, the ratio between saturated and unsaturated permeability decreases as the volume fraction of beads increases, indicating that capillarity effects may decrease due to blocked flow channels between the fabric layers.

1. Introduction

In Liquid Composite Molding (LCM) processes, fabric preforms are cut and assembled prior to mold closure and resin injection. Several types of inclusions can be introduced at this stage by manual or automated sieving between the layers of fabric prior to injection. These inclusions can be introduced for various purposes, including but not limited to ease of stacking and preforming with powdered binders, or to provide self-healing ability with filled microcapsules [1,2].

Addition of the inclusions affects the structure of empty spaces between the adjacent layers and so alters the permeability characteristics of fabrics for resin flow [3–5]. The aim of this work is to investigate the effect of rigid spherical inclusions on the in-plane permeability of fabric preforms and to characterize the influence of the concentration and the size of the particles on the permeability.

Excerpt from ISBN 978-3-00-053387-7

2. Materials

The reinforcement was a woven twill 2x2 E-glass fabric (Suter Kunststoffe AG) with a superficial density (ρ_{sup}) of 390 g/m^2 and a bulk fiber density (ρ_{bulk}) of 2.60 g/cm^3. Interbundle gap ($h_{interbundle}$) as well as the width of fiber bundles of the fabric in weft direction were measured by optical microscopy and shown in Fig. 1. In the base experiment set, 8 layers with in-plane dimensions of 260 mm (weft) x 60 mm (warp) were placed on the mold as depicted in Fig. 2, and compacted to a thickness (h) of 3 mm. Fiber volume fraction (V_f) corresponding to this architecture is calculated as:

$$V_f = \frac{n\rho_{sup}}{h\rho_{bulk}} \tag{1}$$

where n is the number of layers, the corresponding V_f is 40.0%, and porosity (ϕ) is thus,

$$\phi = 1 - V_f \tag{2}$$

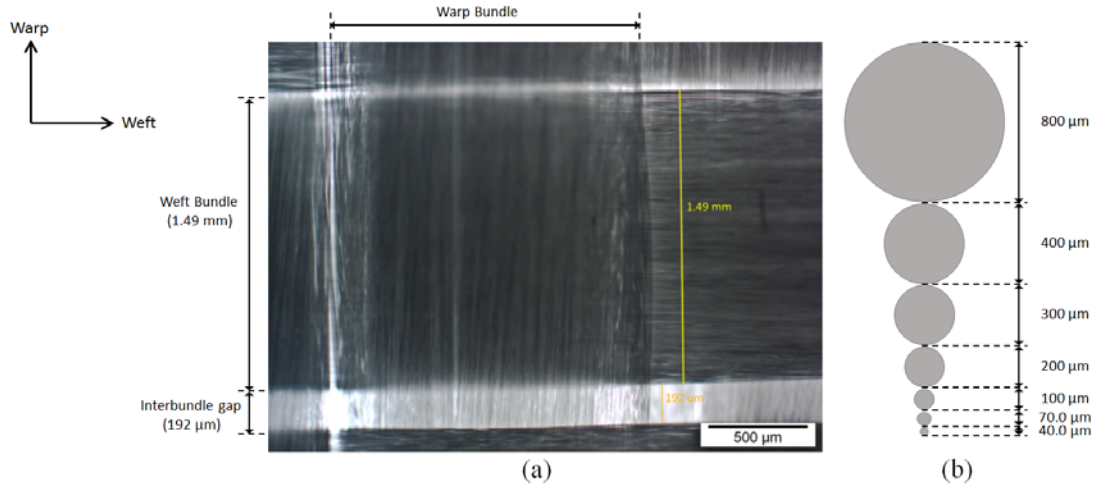

Figure 1. (a) Optical microscopy image showing the typical bundle dimension in weft direction and interbundle gap, (b) representative inclusions scaled to the optical microscopy image.

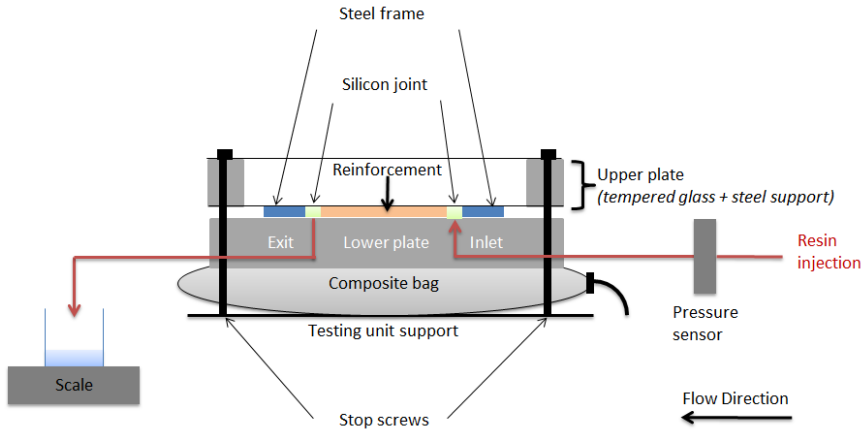

Figure 2. In-plane permeability measurement setup and its components.

Excerpt from ISBN 978-3-00-053387-7

Glass beads (Microbeads AG) were used as model inclusions in this study and were manually sieved between the adjacent layers for various diameter ranges (40.0-70.0, 70.0-100, 100-200, 200-300, 300-400, and 400-800 µm) and concentrations (2.5, 5.0 and 10% bead volume fraction (V_b)). Table 1 presents all the combinations of diameter and concentrations for which experiments were conducted. In the presence of beads, porosity is calculated as

$$\phi = 1 - V_f - V_b. \tag{3}$$

The test fluid was polyethylene glycol (PEG, Sigma Aldrich, 35000 molar mass) diluted in distilled water to reach a viscosity of 100 mPa.s. Viscosity as well as the Newtonian behavior of PEG solution was verified prior to permeability experiments.

Table 1. Volume fractions and diameter ranges in the permeability experiments. Red boxes correspond to the combinations of diameter ranges and volume fractions used in this study.

		Bead Volume Fraction, V_b [%]		
		2.5%	**5.0%**	**10%**
Bead Diameter, d_b [µm]	**40-70**			
	70-100			
	100-200			
	200-300			
	300-400			
	400-800			

3. Methods

Permeability experiments were conducted according to the guidelines detailed in the recent round-robin permeability studies [6] for 1D flow with constant pressure boundary condition, except that the type of the model fluid is different here. In this approach, unsaturated permeability is calculated by following Squared Flow Front (SFF) approach [7]:

$$K_{uns} = \frac{x_{ff}^2\, \phi\, \mu}{2\, P_{inj}\, t} = \frac{m\, \phi\, \mu}{2\, P_{inj}} \tag{4}$$

where x_{ff} is the flow front location, μ is the resin viscosity, P_{inj} is the resin injection pressure, t is time and m corresponds to the slope of x_{ff}^2 vs. t curve. P_{inj} is recorded by placing a Keller S35X piezoresistive transmitter (0 - 10 bar, 0.02 bar accuracy) between the pressure pot and resin inlet. Flow progression was recorded using a Canon EOS 650D camera, and x_{ff} vs. t curve was constructed by tracking the flow front locations and recording arrival times to locations with an interval of 10 mm along the flow direction up to x_{ff} = 260 mm. For calculation of saturated permeability, mass at the exit was recorded using a Mettler Toledo PM2500 scale with an accuracy of 0.001 g at a data acquisition rate of 8 Hz. Mass flow rate was calculated using the acquired mass and time data, and along with the density of resin, it was used for calculating the volumetric flow rate (Q). The following equation was used to calculate the saturated permeability

Excerpt from ISBN 978-3-00-053387-7

$$K_{sat} = \frac{Q\,\mu\,L}{A\,P_{inj}} \tag{5}$$

where L is the specimen length (260 mm), A is the cross-sectional area (60 mm x 3 mm).

In an attempt to determine the permeability in a range of fiber volume fractions, the experiment initially conducted at h = 3.00 mm was repeated for h = 2.80 and 2.50 mm, and the following exponential relation between K and V_f (a first order polynomial relation between $\log K$ and V_f) was fitted to the experimental data

$$K = Ae^{-bV_f} \tag{6}$$

by a least-square method thus determining the constants A and b.

4. Results

In this study, all experiments were conducted in the weft direction and repeated three times. The results of saturated and unsaturated permeability of the plain fabric are presented in Table 2, while the results of the experiments with beads are presented in Table 3.

Eq. 6 is fitted to the unsaturated permeability values as detailed in the previous section, and the constants are found to be A = 1.04×10^{-11} m^2 and b = 18.1. The corresponding curve fit is presented in Fig. 3, along with the experimental results for the plain fabrics and bead-added fabrics.

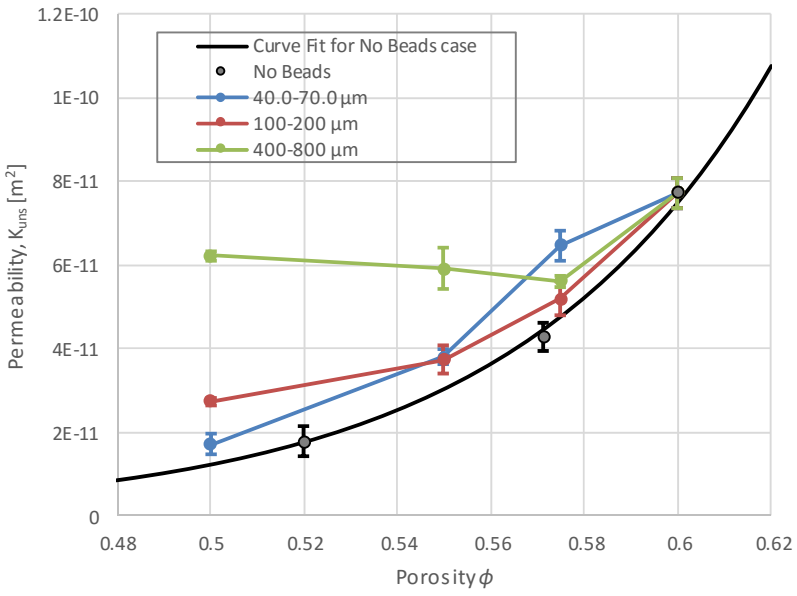

Figure 3. Permeability of plain and bead-added fabrics in terms of porosity. Porosity is calculated using Eq. 2 and Eq. 3 for plain and bead-added fabrics, respectively. Curve fit for no beads case is obtained by using Eq. 6.

Excerpt from ISBN 978-3-00-053387-7

Table 2. Saturated and unsaturated permeability of the plain fabric (with no beads).

	h = 2.50 mm	h = 2.80 mm	h = 3.00 mm
	V_f = 48.0%	V_f = 42.9%	V_f = 40.0%
K_{uns} [×10^{-11} m^2]	1.79 ± 0.348	4.27 ± 0.330	7.72 ± 0.378
K_{sat} [×10^{-11} m^2]	1.66 ± 0.315	3.20 ± 0.272	6.89 ± 0.124

Table 3. Saturated and unsaturated permeability of the fabric in the presence of beads. Results with the gray and white background shading correspond to unsaturated (K_{uns}) and saturated (K_{sat}) permeability, respectively with a unit of 10^{-11} m^2.

		Bead Volume Fraction, V_b [%]		
		2.5	5.0	10
Bead Diameter, d_b [µm]	40-70	6.47 ± 0.361	3.80 ± 0.189	1.72 ± 0.239
		5.66 ± 0.416	3.51 ± 0.136	1.61 ± 0.277
	70-100		3.66 ± 0.093	
			3.23 ± 0.085	
	100-200	5.19 ± 0.407	3.74 ± 0.345	2.75 ± 0.095
		4.31 ± 0.105	3.38 ± 0.282	2.62 ± 0.087
	200-300		5.11 ± 0.551	
			4.91 ± 0.380	
	300-400		5.64 ± 0.115	
			5.16 ± 0.078	
	400-800	5.62 ± 0.132	5.92 ± 0.488	6.23 ± 0.119
		5.26 ± 0.195	5.65 ± 0.404	5.95 ± 0.098

4.1 Effect of inclusion volume fraction, V_b

Fig. 3 illustrates the relationship between the permeability and the bead volume fraction for three bead diameter ranges (40.0-70.0, 100-200, and 400-800 µm), in addition to the permeability of plain fabrics as a function of porosity. For brevity, only the unsaturated permeability is investigated in this section; nevertheless, it should be noted that the trend is similar for saturated permeability..

Here, ϕ is calculated using Eq. 3 and ϕ = 0.60 corresponds to the base experiment with plain fabric. Permeability decreases as V_b increases, thus ϕ decreases, for the beads that are smaller than $h_{interbundle}$ (200 µm). However, for beads with a diameter range of 400-800 µm (which are bigger than $h_{interbundle}$), a non-monotonic relationship between V_b and permeability is observed (see Fig. 3).

During the experiments, it was observed that the beads have a tendency to roll down to the areas at the intersection of warps and wefts. This indicates that the small beads accumulate in these favorable regions and block the existing flow channels between the adjacent layers of fabric. Thus, the permeability of the fiber structure with embedded beads decreases. However, for the large beads, two mechanisms with opposite effects act on the permeability: (1) beads block the existing channels, resulting in a decrease in permeability, and (2) beads deform the structure of the empty channels

Excerpt from ISBN 978-3-00-053387-7

between fiber bundles, resulting in an increase in permeability. The latter of these two mechanisms becomes more influential for high V_b values (see Fig. 3), indicating that formation of new flow channels by deformation of the adjacent fabric layers dominates the blocking of the existing channels around the intersection of warps and wefts.

4.2 Effect of inclusion diameter, d_b

To further investigate the influence of bead diameter on permeability, Fig. 4 reports the permeability as a function of bead diameter for three V_b values (2.5, 5.0, and 10%). It is difficult to reach a conclusion for 2.5% curve. The curve for 10% is in agreement with our conclusions of the previous section. The curve for 5.0% reveals that, for a fixed volume fraction of beads, the permeability decreases more significantly when $d_b < h_{interbundle}$ than for beads with $d_b > h_{interbundle}$, where $h_{interbundle}$ is approximately 200 µm. It should also be noted that the permeability is in the same range for the small d_b cases (40.0 – 70.0, 70.0 – 100, 100 – 200 µm), whereas it significantly increases as d_b increases for $d_b > h_{interbundle}$ cases (200 – 300, 300 – 400, 400 – 800 µm).

As discussed in the previous section, beads have two opposite deformation mechanisms on the fabric structure's permeability. For small beads, the formation of new channels is insignificant, whereas for large beads, formation of new channels and blocking of existing channels may happen simultaneously.

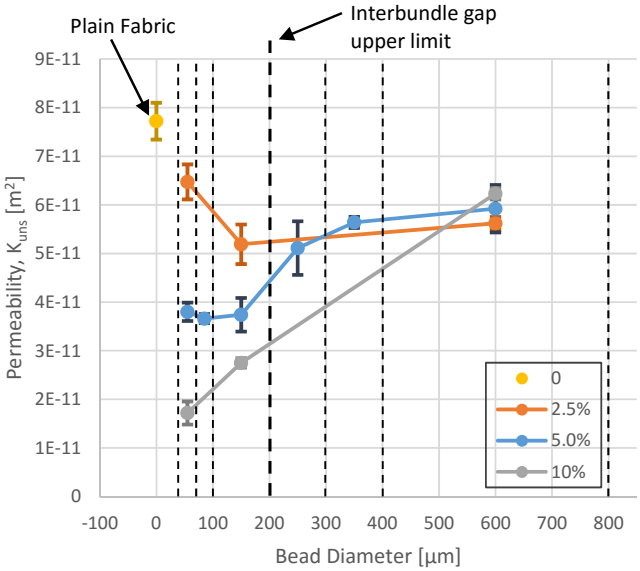

Figure 4. Unsaturated permeability as a function of bead diameter, d_b. Vertical dashed lines show the lower and upper bounds for each diameter range. 0 bead diameter corresponds to the permeability of plain fabric.

4.3 Role of capillarity

The ratio of unsaturated to saturated permeability, $R_s = K_{unsat}/K_{sat}$ is a straightforward indicator whether the test fluid behaves as a wetting fluid ($R_s > 1$) or as a non-wetting fluid ($R_s < 1$) for a specific type of fabric [8].

Excerpt from ISBN 978-3-00-053387-7

In all of the 15 experiment sets in this study, which were conducted with an injection pressure ranging between 0.9 bar and 1.0 bar, R_s was higher than unity, indicating that the PEG solution behaved as a wetting fluid. The relationship between V_b and R_s for the three bead diameter ranges is presented in Fig. 5. For all the diameter ranges, R_s decreases as V_b increases, indicating that the effect of capillary forces are reduced, possibly due to the blocking of channels by the added beads, making the porosity distribution more uniform. The decrease in R_s for large beads is smaller compared to that of small beads and this is in agreement with our previous conclusions that existing channels are blocked by small beads, whereas new channels are formed by deformation of fabrics in addition to blocking of some existing channels by large beads.

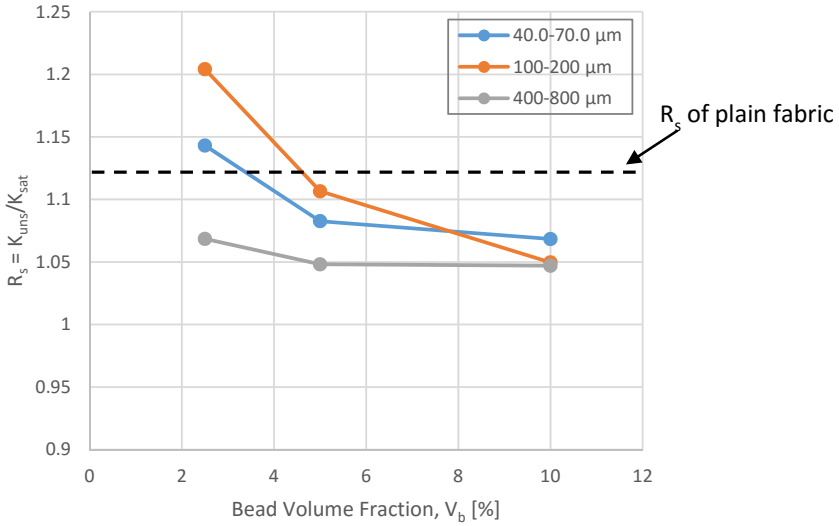

Figure 5. Ratio of unsaturated permeability to saturated permeability, R_s, as a function of bead volume fraction, V_b.

5. Conclusions

In this ongoing work, the effect of inclusions (model beads) on fabric permeability was investigated by conducting multiple experiments with several bead diameter ranges (40.0-70.0, 70.0-100, 100-200, 200-300, 300-400, and 400-800 µm) and several bead volume fractions (2.5, 5.0, and 10%).

Results indicated that $h_{interbundle}$ acts as a threshold value in determining the effect of inclusions on permeability. For beads smaller than $h_{interbundle}$, permeability continued to decrease as V_b increased since the channels became blocked from the accumulation of beads. On the other hand, for larger beads, an increase in permeability was observed as V_b increased due to formation of new channels.

An investigation on the relationship between saturated and unsaturated permeability showed that the test fluid behaved as wetting fluid in all experiments and the effect of capillarity was reduced as V_b is increased. Further work is ongoing with different test fluids and activated bead surfaces to further reveal the role of capillary effects.

Excerpt from ISBN 978-3-00-053387-7

Acknowledgements

B. Caglar acknowledges the support through a Swiss Government Excellence Scholarship for the academic year 2015-2016.

References

[1] Rohatgi V, Lee LJ. Moldability of tackified fiber preforms in liquid composite molding. J Compos Mater 1997;31:720–44.

[2] Manfredi E, Michaud V. Packing and permeability properties of E-glass fibre reinforcements functionalised with capsules for self-healing applications. Compos Part A Appl Sci Manuf 2014;66:94–102.

[3] Estrada G, Vieux-Pernon C, Advani SG. Experimental characterization of the influence of tackifier material on preform permeability. J Compos Mater 2002;36:2297–310.

[4] Dickert M, Ziegmann G. Influence of binder on the mechanical properties and the permeability of a non-crimp carbon fabric preform 2012:24–8.

[5] Nordlund M, Fernberg SP, Lundström TS. Particle deposition mechanisms during processing of advanced composite materials. Compos Part A Appl Sci Manuf 2007;38:2182–93.

[6] Arbter R, Beraud JM, Binétruy C, Bizet L, Bréard J, Comas-Cardona S, et al. Experimental determination of the permeability of textiles: A benchmark exercise. Compos Part A Appl Sci Manuf 2011;42:1157–68.

[7] Vernet N, Ruiz E, Advani SG, Alms JB, Aubert M, Barburski M, et al. Experimental determination of the permeability of engineering textiles: Benchmark II. Compos Part A Appl Sci Manuf 2014;61:172–84.

[8] Michaud V. A review of non-saturated resin flow in liquid composite moulding processes. Transp Porous Media 2016.

Excerpt from ISBN 978-3-00-053387-7